SUPPLEMENT TO

Trends, composition and sources of carbonaceous aerosol in the last 18 years at the Birkenes Observatory, Northern Europe, by K. E. Yttri et al.

S1. Quality assurance

The OC/EC data are not field blank corrected, in accordance with the standard operating procedure provided by EMEP (Yttri et al., 2007a; EMEP, 2014). The positive sampling artefact of OC for weekly samples collected at Birkenes has been quantified on a campaign basis using the QBQ (Quartz fibre filter Behind Quartz fibre filter) approach (McDow and Huntzicker, 1990; Turpin et al., 1994) in summer (18±4%; Yttri et al., 2011), fall (19±7%; Yttri et al., 2019), and winter/spring (24±13%; Yttri et al., 2019) but only for PM_{10}. For OC in $PM_{2.5}$, which at Birkenes is obtained from an identical and co-located sampler, operating at the same filter face velocity as the PM_{10} sampler, the positive sampling artefact is considered equally large, whereas its relative importance is slightly higher. The negative sampling artefact has not been addressed.

OC/EC analysis was performed within 2 months after the filter samples were collected and according to the Quartz (2001–2008) and the EUSAAR-2 (from 2008) temperature programs. EUSAAR-2 is designed to reduce the inherited uncertainties associated with splitting of OC and EC, e.g. by preventing premature burn-off of EC (Cavalli et al., 2010). The uncertainty associated with repeated OC/EC analyzes of a filter sample is typically <10%, which includes both analytical uncertainty and heterogenic distribution of the deposited aerosol particles on the filter sample.

The laser´s ability to detect changes in the transmittance of a filter sample high in initial EC is crucial to obtain a correct value for EC (and OC). 15 µg EC cm^{-2} has been suggested as an upper limit (Subramanian et al., 2006; Wallén et al., 2010) but this value is likely to vary. The nine filter samples (out of nearly 1800) with an EC content exceeding 15 µg C cm^{-2} in the current dataset were considered valid. Further, a non-biased separation between OC and EC requires that either pyrolytic carbon (PC) evolves before EC during analysis or that PC and EC have the same light absorption coefficient. It is well known that this is not always the case (Yang and Yu, 2002) and there is a lack of information on the magnitude of this imperfection.

Deviation from the protocol-defined temperature steps will affect the analysis results of the TOA instrument (Chow et al., 2005; Panteliadis et al., 2015) and temperature offsets ranging from -93 °C to +100 °C per temperature step have been reported (Panteliadis et al., 2015). Thus, calibration by the temperature calibration kit available from the instrument manufacturer (Sunset laboratory Inc) since 2012 is strongly recommended. Temperature calibration was implemented as part of the regular QA/QC procedures for thermal-optical analysis in 2013.

A comparison of the two temperature programmes used for the Birkenes time series was performed for $PM_{2.5}$ filter samples collected at Birkenes in 2014, using temperature calibrated versions of both Quartz and EUSAAR-2. There was a good agreement between the two temperature programs for TC and OC, i.e. close to the expected uncertainty associated with analysis and sampling, whereas for EC the difference was pronounced (Table S 17), although in close correspondence with that previously reported by Panteliadis et al. (2015). Note that OC and EC data for the period 2001–2007 discussed in the main is text not corrected according to Eq. (S 18–20) (Table S 17), except for the purpose of trend calculations.

Field blanks did not contain monosaccharide anhydrides, sugars, sugar-alcohols or 2-methyltetrols in noticeable amounts. Filter samples for which the content was below the LOD but > 0, were considered valid and included when calculating the annual and seasonal means. Organic tracers were analyzed within 1 year after collection of the aerosol filter samples. The uncertainty (analytical and sampling uncertainty) associated with measurements of monosaccharide anhydrides is within 10 – 15 % (Yttri et al., 2015). A similar range of uncertainty is expected for the other organic tracers.

Mass concentrations of PM_{10} and $PM_{2.5}$ were field blank corrected. The overall uncertainty associated with determination of the PM_{10} and $PM_{2.5}$ mass concentration is < 5%. The monitoring of major ions and trace elements follows the guidelines by EMEP (EMEP, 2014) and are within the data quality objective of the network: 15–25% uncertainty for the combined sampling and analysis of major ions and 30% for heavy metals.

S2. Calculation of trends - Statistical approach

The Mann-Kendall test (Mann, 1945; Kendall, 1975; Gilbert, 1987) was used for calculating the significance of the trend and if a significant trend was found, the Theil-Sen slope (Theil, 1958; Sen, 1968; Gilbert, 1987) was calculated. This procedure has been widely used in atmospheric science, like in the recent TOAR project analysing global surface ozone trends (e.g. Fleming et al., 2018; Lefohn et al., 2018), in the review of the EMEP observations (Tørseth et al., 2012) and in numerous other observation based papers (Aas et al. 2019; Ciarelli et al., 2019; Theobald et al., 2019; Masiol et al., 2019; Collaud Coen et al., 2020).

The Mann-Kendall test is a non-parametric test that does not rely on any assumptions of distribution and is therefore well suited for atmospheric data that often deviates from normality and contain outliers that would hamper a standard linear regression. The basics of the Mann-Kendall test is to count the signs of all forward concentration differences in time, and if there is a sufficient overweight of positive or negative differences, the 0-hypothesis (H_0) of no trend could be rejected. The S statistic given below contains the sum of all the signs based on the observed values y_i at time *i*:

$$S = \sum_{1=1}^{n-1} \sum_{j=i+1}^{n} sign\left(y_j - y_i\right) \qquad Eq.S1$$

This statistic together with the number of samples and the number of ties in the data were used to calculate the p value as given by Gilbert (1987). In our work, we assumed significant trends when $p <$ 0.05.

With $p < 0.05$ H_0 was rejected and the value of the trend was estimated by the Theil-Sen slope estimator:

$$\beta = median\left(\frac{y_j - y_i}{t_j - t_i}\right), \qquad j > i \qquad Eq.S2$$

where t_i denotes the time i of the observed value y_i.

The Theil-Sen slope is simply the median of all the forward concentration gradients. In addition to the slope, the 2σ confidence intervals were calculated according to Gilbert (1987), providing the 95 % confidence range of the slopes.

The Mann-Kendall test and Theil-Sen slope estimation was applied to all species and ratios discussed in this work. These calculations were based on the seasonal and annual mean values, separately, as presented below. For the ratios, r = x/y (e.g. the fraction of NO_3^- in PM_{10}), we based the calculations on the ratios of the seasonal means and not on the seasonal means of the ratios, i.e.:

$$r = \frac{x}{y}, where\ x = \frac{1}{n}\sum(x_i)\ and\ y = \frac{1}{n}\sum(y_i) \qquad Eq.S3$$

For all cases where the 0-hypothesis (H_0) could be rejected, the Theil-Sen slopes were calculated, and this slope was further transferred into the relative trend by dividing the trend (β) by the mean of the observed values:

$$\beta_{rel} = \frac{\beta}{\left[\frac{1}{n}\sum(y_i)\right]}\ , where\ y_i = observed\ concentration\ or\ ratio\ at\ time\ i \qquad Eq.S4$$

S3. Absorption coefficent measurements and source apportionment

The absorption coefficient (B_{Abs}) was measured using the multi wavelength (λ=370; 470; 520; 590; 660; 880; 950 nm) aethalometer (AE33, Magee Scientific), operating behind a PM_{10} inlet. We calculate absorption coefficients (B_{Abs}) according to Drinovec et al. (2015):

$$B_{Abs}(\lambda) = \frac{A\cdot\left(\frac{ATN_{t2}(\lambda) - ATN_{t1}(\lambda)}{100}\right)}{Q\cdot C\cdot(1-\zeta)\cdot\left(1 - k(\lambda)\cdot\left(ATN_{t2}(\lambda) - ATN_{ref}(\lambda)\right)\right)\cdot(t_2 - t_1)} \qquad Eq.\mathrm{S5}$$

where ATN = attenuation at time t =1 and t =2, and of the reference spot *ref*, Q is the instrument flow rate on spot 1, A is the filter spot area, k is the loading compensation parameter from the 2 spot compensation algorithm. Here we neglect lateral air flow losses (ζ) and the scattering compensation C

since these are not wavelength dependent in Eq. (S5) and hence do not affect source apportionment based on wavelength dependence, while conversion to eBC via co-located filter measurements of EC also results in compensation of these parameters using:

$$\mathrm{eBC}(\lambda) = B_{Abs}(\lambda) / \alpha_{\mathrm{effective}}(\lambda) \qquad Eq.S6$$

where $\alpha_{\mathrm{effective}}$ is an effective mass absorption cross section (α) incorporating scattering and lateral flow losses:

$$\alpha_{effective}(\lambda) = \alpha(\lambda) \times c \times (1 - \zeta) \qquad Eq.S7$$

Hence $\alpha_{effective}$ is a conversion factor between B_{Abs} and eBC and has no physical meaning beyond this.

The AE33 of this study automatically generates $B_{Abs}(\lambda)$ at 1-minute resolution. However, as discussed by of Springston et al. (2007) and Backmann et al. (2017), the time interval $(t_2 - t_1)$ Eq.(S5) can be adjusted to any integer multiple of the base resolution in post-processing. Here we adapt the approach of Backmann et al. (2017), fixing the time interval to 1 hour and calculating $B_{Abs}(\lambda)$ according to Eq. (S5). In case one or more filter advances occurred within the one-hour interval, data from each individual filter spot falling within the interval were treated separately and a time-weighted average recorded for that hour. The advantage of this technique is enhanced noise reduction, i.e. using the one-hour interval approach the noise reduction is proportional to as much as *1/n* (where *n* are the measurement points), rather than *1/sqrt(n),* attainable via signal averaging.

Here we performed source apportionment of aethalometer data using the *aethalometer model* (Sandradewi et al., 2008). Assuming two sources contribute to total Babs ($B_{Abs,Tot}$), i.e. fossil fuel combustion ($B_{Abs,ff}$) and biomass burning ($B_{Abs,bb}$):

$$B_{Abs,Tot} = B_{Abs,ff} + B_{Abs,bb} \qquad Eq.\ S8$$

Then, using a wavelength pair, here λ_1=470 nm and λ_2=880 nm,

$$B_{Abs,bb}(\lambda_2) = \frac{B_{Abs}(\lambda_1) - B_{Abs}(\lambda_2) \cdot \left(\frac{\lambda_1}{\lambda_2}\right)^{-\alpha_{ff}}}{\left(\frac{\lambda_1}{\lambda_2}\right)^{-\alpha_{bb}} - \left(\frac{\lambda_1}{\lambda_2}\right)^{-\alpha_{ff}}} \qquad Eq.\ S9 \text{ and}$$

$$B_{Abs,ff}(\lambda_2) = \frac{B_{Abs}(\lambda_1) - B_{Abs}(\lambda_2) \cdot \left(\frac{\lambda_1}{\lambda_2}\right)^{-\alpha_{bb}}}{\left(\frac{\lambda_1}{\lambda_2}\right)^{-\alpha_{ff}} - \left(\frac{\lambda_1}{\lambda_2}\right)^{-\alpha_{bb}}} \qquad Eq.\ S10$$

where α_{ff} and α_{bb} are the absorption Ångstrøm exponents (AAE) for fossil fuel and biomass burning, respectively. Note that when using this approach, the AAEs must be assumed *a priori,* while the data are not fitted or error weighted, which can lead to negative values in the resulting time series of the factors due to uncertainty in the AAEs e.g. Grange et al. (2020).

Here we also used positive matrix factorisation (PMF) to distinguish between the two sources in Eq. (S8). The theory of PMF is detailed elsewhere (Paatero et al., 1994) Briefly, a matrix of measurement data *X* is represented by a bilinear model comprising factor profiles *F* (rows), factor time series G (columns) and a residual matrix E:

$$X = G \cdot F + E \qquad \textit{Eq. S11}$$

In PMF factors are found using a least-squares fitting routine in which the object function Q, i.e. the square of residuals e weighted to uncertainty σ, is mimimised across all cells (rows i-m, columns j-n)

$$Q^m = \sum_{i=1}^{m} \sum_{j=1}^{n} \left(\frac{e_{ij}}{\sigma_{ij}}\right)^2 \qquad \textit{Eq.}\ \text{S12}$$

Here, we use the source finder (SoFi, (Canonaco et al., 2013)) toolkit ref, to call PMF (To model the error matrix σ_{ij} we use the clean air test function of the AE33 to determine the standard deviation of the attenuation of the blank $\delta_{ATN_{air}}$, calculating σ_{ij}, using:

$$\sigma_{ij} = \sqrt{f_A^2 + f_Q^2 + 2\left(\frac{\delta_{ATN_{air}}(\lambda_j)}{ATN_i(\lambda_j)}\right)^2 + \left(\frac{\delta_{ATN_{air}}(\lambda_j)}{ATN_{i-1}(\lambda_j)}\right)^2 + \left(\frac{\delta_{ATN_{air}}(\lambda_j)}{ATN_{ref}(\lambda_J)}\right)^2} \cdot B_{Abs,i}(\lambda_j) \qquad Eq. S13$$

where f_A and f_Q are the fractional uncertainties in the spot area and the flow rate, respectively (both 0.015 according to Backman et al., 2017). Clean air tests were performed only periodically. Therefore, to generate an error estimate for all time points, we interpolated (bilinear interpolation) between the clean air tests to generate the full error matrix, accounting for drift in $\delta_{ATN_{air}}$. Points before and after the last clean air test were calculated using the first and last values of $\delta_{ATN_{air}}$, respectively.

According to Eq. (S11), X could be represented by any combination of G and F, i.e. the PMF model has *rotational ambiguity*. In practice, many rotations produce negative values and are thus forbidden. Nevertheless, many rotations and local minima in Eq. (S11) are likely to exist. To assess this, we generated multiple (*n*=2000) bootstrap replacement matrices (block size 24 to conserve diurnal variation if present), running PMF on each matrix 5 times for a total of 10000 runs. PMF settings are shown in Table S 2.

We import all 2000 files generated using SoFi for each factor solution. To map the factors, we calculated an effective AAE from the factor profiles α_F, using

$$\alpha_F = -\frac{\log\left(F_{j=2}/F_{j=6}\right)}{\log(470/880)} \qquad Eq. S14$$

sorting factors and time series from each run from low to high with respect to α_F. Binning the effective AAEs from each factor also provides a convenient means to investigate the solution space for rotational ambiguity.

S4. Positive matrix factorisation applied to filter data

We performed PMF with the following as input data: OC (in $PM_{2.5}$ and $PM_{10-2.5}$), EC (in PM_{10}), levoglucosan, mannosan, galactosan, arabitol, mannitol, trehalose, glucose, V, Mn, Ti, Fe, Co, Ni, Cu, Zn, As, Cd, and Pb (all in PM_{10}), SO_4^{2}, NO_3^-, NH_4^+, Ca^{2+}, Mg^{2+}, K^+, Na^+, Cl^- (open filter face). Table S 3 shows miscellaneous settings of the PMF analysis of these data. The input data and error estimates were prepared using the procedure suggested by Polissar et al. (1998) and Norris et al. (2014), see also Table S 3 for miscellaneous settings including missing data treatment and assessment of the PMF performance.

If the concentration was greater than the LOD, the calculation was based on a user provided fraction of the concentration and LOD:

$$Unc = \sqrt{(Error\ Fraction \times Concentration)^2 + (\frac{1}{2} \times LOD)^2} \qquad Eq.S15$$

The analytical uncertainties (20%) as error fraction of OC, EC, organic tracers, ions, and elements were used to determine the corresponding error estimates. Based on given understanding of OC sources, 2–10 factors with random seeds were examined, and 7 factors were determined based on: 1) The decrease in Q/Qexp was larger than the relative change in number of factors up to 7; 2) All factors could be interpreted; 3) All factors were distinct.

To assess the statistical uncertainty in the model we performed repeated analyses on bootstrap-resampled matrices. A base profile was generated from a manually mapped average of 50 runs. From each bootstrap run, we fitted all 7 bootstrap factors vs all 7 factors from the base run profile (representing a 7×7 matrix of r^2 values). We then mapped the bootstrap factors in order of the r^2 value: The highest value was assumed to be a match, then then the next highest value excluding both previously mapped factors to any other factor (representing a 6×6 matrix of r^2 values) , and so on. This was to avoid any factors being mapped twice.

The minimal robust and true Q values of the base run were 5507.9 and 5580.8, respectively. All the (error) scaled residuals were within ±5 and > 97.8% within ± 3, normally distributed and centred around zero. The average Q/Qexp was 1.2. We also observe no structure in the residuals, which were evenly distributed between measurements from different instruments (i.e. we did not observe factors representing groups of compounds by instrument type, Figure S 3).

S5. Emission ratios used to calculate OC and EC from biomass burning

Emission ratios derived from ambient data are a good alternative to direct emission measurements, accounting for the aggregate effects of fuel type and combustion conditions, but results will nevertheless vary from region to region (e.g. Zotter et al., 2014). Here, we used ratios from our PMF analysis (Table 1) to calculate carbonaceous aerosol from biomass burning for 2008–2018. The levoglucosan to mannosan ratio is rather consistent between seasons, with the values for summer (5.1±0.9) and fall (5.2±0.7) being slightly lower than for winter (5.4±0.8) and spring (6.0±0.7). This might indicate that emissions from one source of biomass burning (wood burning for residential heating) dominate for all seasons, supporting the use of one levoglucosan to OC (and EC) ratio for calculations. The lower levoglucosan to mannosan ratio observed in summer and fall might indicate increased influence of wild and agricultural fires, but the magnitude of these sources remains speculative, except during severe episodes, e.g. in August 2002, May and September 2006, and June 2008.

S6. Levels of PBAP and BSOA organic tracers

The annual mean concentration of the PBAP tracers ranged from 2.8–3.4 ng m^{-3} (trehalose) to 4.8–5.8 ng m^{-3} (arabitol) (2016–2018) (Figure 6, Table S 15). Levels were elevated in the vegetative season, particularly in summer and fall. Mannitol and arabitol were highly correlated (R^2=0.85), underlining their common origin, and the mannitol to arabitol ratio (0.9±0.2) corresponds well with previously reported results for these fungal spore tracers (e.g. Bauer et al., 2008a; Yttri et al., 2007b; Yttri et al. 2011 a, b).

The annual mean concentration of 2-methylerythritol (0.365–0.441 ng m^{-3}) (2016–2018) was higher than that of 2-methylthreitol (0.105–162 ng m^{-3}), and the two isomers were highly correlated (R^2=0.915), which is consistent with other studies (e.g., Ion et al., 2005; Kourtchev et al., 2005; Edney et al., 2005; El Haddad et al., 2011; Alier et al., 2013). 2-methyltetrols were elevated in the period when deciduous trees have leaves (transition May/June to early October).

References Supplementary

Alier et al., 2013: Atmos. Chem. Phys., 13, 10353–10371, 2013 www.atmos-chem.phys.net/13/10353/2013/doi:10.5194/acp-13-10353-2013.

Backman, J., Schmeisser, L., Virkkula, A., Ogren, J. A., Asmi, E., Starkweather, S., Sharma, S., Eleftheriadis, K., Uttal, T., and Jefferson, A. J. A. M. T.: On Aethalometer measurement uncertainties and an instrument correction factor for the Arctic, A, 2017.

Canonaco, F., Crippa, M., Slowik, J. G., Baltensperger, U., and Prévôt, A. S. H.: SoFi, an IGOR-based interface for the efficient use of the generalized multilinear engine (ME-2) for the source apportionment: ME-2 application to aerosol mass spectrometer data, Atmos. Meas. Tech., 6, 3649–3661, https://doi.org/10.5194/amt-6-3649-2013, 2013

Chow, J. C., Watson, J. G., Chen, L.-W. A., Paredes-Miranda, G., Chang, M.-C. O., Trimble, D., Fung,

K. K., Zhang, H., and Yu, J. Z.: Refining temperature measures in thermal/optical carbon analysis. Atmos. Chem. Phys., 5, 2961–2972, 2005.

Ciarelli, G., Theobald, M. R., Vivanco, M. G., Beekmann, M., Aas, W., Andersson, C., Bergström, R., Manders-Groot, A., Couvidat, F., Mircea, M., Tsyro, S., Fagerli, H., Mar, K., Raffort, V., Roustan, Y., Pay, M.-T., Schaap, M., Kranenburg, R., Adani, M., Briganti, G., Cappelletti, A., D'Isidoro, M., Cuvelier, C., Cholakian, A., Bessagnet, B., Wind, P., and Colette, A.: Trends of inorganic and organic aerosols and precursor gases in Europe: insights from the EURODELTA multi-model experiment over the 1990–2010 period, Geosci. Model Dev., 12, 4923–4954, 2019, https://doi.org/10.5194/gmd-12-4923-2019.

Collaud Coen, M., Andrews, E., Alastuey, A., Arsov, T. P., Backman, J., Brem, B. T., Bukowiecki, N., Couret, C., Eleftheriadis, K., Flentje, H., Fiebig, M., Gysel-Beer, M., Hand, J. L., Hoffer, A., Hooda, R., Hueglin, C., Joubert, W., Keywood, M., Kim, J. E., Kim, S.-W., Labuschagne, C., Lin, N.-H., Lin, Y., Lund Myhre, C., Luoma, K., Lyamani, H., Marinoni, A., Mayol-Bracero, O. L., Mihalopoulos, N., Pandolfi, M., Prats, N., Prenni, A. J., Putaud, J.-P., Ries, L., Reisen, F., Sellegri, K., Sharma, S., Sheridan, P., Sherman, J. P., Sun, J., Titos, G., Torres, E., Tuch, T., Weller, R., Wiedensohler, A., Zieger, P., and Laj, P.: Multidecadal trend analysis of in situ aerosol radiative properties around the world, Atmos. Chem. Phys., 20, 8867–8908, https://doi.org/10.5194/acp-20-8867-2020, 2020

Drinovec, L., Močnik, G., Zotter, P., Prévôt, A., Ruckstuhl, C., Coz, E., Rupakheti, M., Sciare, J., Müller, T., and Wiedensohler, A. J. A. M. T.: The" dual-spot" Aethalometer: an improved measurement of aerosol black carbon with real-time loading compensation, 8, 1965-1979, 2015.

Edney, E. O., Kleindienst, T. E., Jaoui, M., Lewandowski, M., Offenberg, J. H., Wang, W., and Claeys, M.: Formation of 2-methyltetrols and 2-methylglyceric acid in secondary organic aerosolfrom laboratory irradiated isoprene/NO_x/SO_2/air mixtures and their detection in ambient $PM_{2.5}$ samples collected in the eastern United States, Atmos. Environ., 39, 5281–5289, 2005.

El Haddad, I., Marchand, N., Temime-Roussel, B., Wortham, H., Piot, C., Besombes, J.-L., Baduel, C., Voisin, D., Armengaud, A., and Jaffrezo, J.-L.: Insights into the secondary fraction of the organic aerosol in a Mediterranean urban area: Marseille, Atmos. Chem. Phys., 11, 2059–2079, https://doi.org/10.5194/acp-11-2059-2011, 2011.

EMEP: Standard Operating Procedures for thermal-optical analysis of atmospheric particulate organic and elemental carbon, in: EMEP manual for sampling and chemical analysis, EMEP/CCC 01/2014, NILU, Kjeller, Norway, chapter 4.22, 2014.

Fleming, Z.L., Doherty, R.M., von Schneidemesser, E., Malley, C.S., Cooper, O.R., Pinto, J.P., Colette, A., Xu, X., Simpson, D., Schultz, M.G., Lefohn, A.S., Hamad, S., Moolla, R. Solberg, S., and Feng, Z.: Tropospheric Ozone Assessment Report: Present-day ozone distribution and trends relevant to human health, Elem Sci Anth, 6: 12. DOI: https://doi.org/10.1525/elementa.273, 2018.

Gilbert, R. O.: Statistical Methods for Environmental Pollution Monitoring, Wiley, NY, United States, pp. 336, 1987.

Grange, S. K., Lötscher, H., Fischer, A., Emmenegger, L., and Hueglin, C.: Evaluation of equivalent black carbon source apportionment using observations from Switzerland between 2008 and 2018, Atmos. Meas. Tech., 13, 1867–1885, https://doi.org/10.5194/amt-13-1867-2020, 2020.

Ion, A. C., Vermeylen, R., Kourtchev, I., Cafmeyer, J., Chi, X., Ge-lencs´er, A., Maenhaut, W., and Claeys, M.: Polar organic com-pounds in rural PM2.5aerosols from K-puszta, Hungary, duringa 2003 summer field campaign: sources and diel variations, At-mos. Chem. Phys., 5, 1805–1814, 2005,SRef-ID: 1680-7324/acp/2005-5-1805.

Kourtchev, T. Ruuskanen, W. Maenhaut, M. Kulmala, and M. Claeys. Observation of 2-methyltetrols and related photo-oxidation products of isoprene in boreal forest aerosols from Hyytiälä, Finland. Atmos. Chem. Phys., 5, 2761–2770, 2005.

Kendall, M. G.: Rank correlation methods, 4th edition, Charles Griffin, London, 1975.

Lefohn, A. S., Malley, C. S., Smith, L., Wells, B., Hazucha, M., Simon, H., Naik, V., Mills, G., Schultz, M. G., Paoletti, E., De Marco, A., Xu, X., Zhang, L., Wang, T., Neufeld, H. s., Musselman, R. C., Tarasick, D., Brauer, M., Feng, Z., Tang, H., Kobayashi, K., Sicard, P., Solberg, S., and Gerosa, G.: Tropospheric ozone assessment report: Global ozone metrics for climate change, human health, and crop/ecosystem research, Elem Sci Anth, 6: 28, DOI: https://doi.org/10.1525/elementa.279, 2018.

Mann, H. B.: Non-parametric tests against trend, Econometrica 13:163-171, 1945.

Masiol, M., Squizzato, S., Rich, D. Q., and Hopke, P. K.: Long-term trends (2005–2016) of source apportioned PM2.5 across New York State, Atmos Environ., 201, 110-120, https://doi.org/10.1016/j.atmosenv.2018.12.038, 2019.

McDow, S. R. and Huntzicker, J. J.: Vapor adsorption artifact in the sampling of organic aerosol: face velocity effects, Atmos. Environ., 24A, 2563–2571, 1990.

Norris, G., Duvall, R., Brown, S., and Bai, S.: EPA Positive Matrix Factorization (PMF) 5.0 Fundamentals and User Guide, U.S. Environmental Protection Agency, Washington, DC, 20460 (i-124, EPA/600/R-14/108, April), 2014.

Paatero, P. and Tapper, U.: Positive Matrix Factorization – A nonnegative factor model with optimal utilization of error-estimates of data values. Environmetrics, 5, 111-126, DOI: 10.1002/env.3170050203, 1994.

Panteliadis, P., Hafkenscheid, T., Cary, B., Diapouli, E., Fischer, A., Favez, O., Quincey, P., Viana, M., Hitzenberger, R., Vecchi, R., Saraga, D., Sciare, J., Jaffrezo, J. L., John, A., Schwarz, J., Giannoni, M., Novak, J., Karanasiou, A., Fermo, P., and Maenhaut, W.: ECOC comparison exercise with identical thermal protocols after temperature offset correction – instrument diagnostics by in-depth evaluation of operational parameters, Atmos. Meas. Tech., 8, 779–792, 2015.

Pio, C. A., Legrand, M., Oliveira, T., Afonso, J., Santos, C., Caseiro, A., Fialho, P., Barata, F., Puxbaum, H., Sanchez-Ochoa, A., Kasper-Giebl, A., Gelencsér, A., Preunkert, S., and Schock, M.: Climatology of aerosol composition (organic versus inorganic) at nonurban sites on a west-east transect across Europe, J. Geophys. Res., 112, https://doi.org/10. 1029/2006JD008038, 2007.

Polissar, A. V., Hopke, P. K., Paatero, P., et al. Atmospheric aerosol over Alaska: 2. Elemental composition and sources. Journal of Geophysical Research: Atmospheres, 103(D15): 19045-19057, 1998.

Sen, P. K.: Estimates of the regression coefficient based on Kendall's Tau. J. Am., Stat. Assoc. 63 (324), 1379–1389.https://doi.org/10.2307/2285891, 1968.

Springston, S. R. and Sedlacek III, A. J.: Noise Characteristics of an Instrumental Particle Absorbance Technique, Aerosol Science and Technology, 41:12, 1110-1116, DOI: 10.1080/02786820701777457, 2007.

Subramanian, R., Khlystov, A. Y., Cabada, J. C., and Robinson, A. L.: Positive and negative artifacts in particulate organic carbon measurements with denuded and undenuded sampler configurations, Aerosol Sci. Tech., 38(S1), 27–48, 2004.

Theil, H.: A rank-invariant method of linear and polynomial regression analysis. Proceedings of the Royal Netherlands, Acad. Sci. 53, 386–392, https://doi.org/10.1007/978-94-011-2546-8_20, 1950.

Theobald, M. R., Vivanco, M. G., Aas, W., Andersson, C., Ciarelli, G., Couvidat, F., Cuvelier, K., Manders, A., Mircea, M., Pay, M.-T., Tsyro, S., Adani, M., Bergström, R., Bessagnet, B., Briganti, G., Cappelletti, A., D'Isidoro, M., Fagerli, H., Mar, K., Otero, N., Raffort, V., Roustan, Y., Schaap, M., Wind, P., and Colette, A.: An evaluation of European nitrogen and sulfur wet deposition and their trends estimated by six chemistry transport models for the period 1990–2010, Atmos. Chem. Phys., 19, 379–405, https://doi.org/10.5194/acp-19-379-2019, 2019.

Turpin, B. J., Huntzicker, J. J., and Hering S. V.: Investigation of organic aerosol sampling artefacts in the Los Angeles basin, Atmos. Environ., 28, 3061–3071, 1994.

Wallén, A., Lidén, G., and Hansson H. C.: Measured Elemental Carbon by Thermo-Optical Transmittance Analysis in Water- Soluble Extracts from Diesel Exhaust, Woodsmoke, and Ambient Particulate Samples, J. Occup. Environ. Med., 7, 35–41, https://doi.org/10.1080/15459620903368859, 2010.

Yang, H. and Yu, J. Z.: Uncertainties in Charring Correction in the Analysis of Elemental and Organic Carbon in Atmospheric Particles by Thermal/Optical Methods, Environ. Sci. Technol., 36, 5199–5204, 2002.

Yttri, K. E, Schnelle-Kreis, K., Maenhaut, W., Abbaszade, G., Alves, C., Bjerke, A., Bonnier, N., Bossi, R., Claeys, M., Dye, C., Evtyugina, M., García-Gacio, D., Hillamo, E., Hoffer, A., Hyder, M., Iinuma, Y., Jaffrezo, J.-L., Kasper-Giebl, A., Kiss, G., López-Mahia, P. L., Pio, C, Piot, C. Ramirez-Santa-Cruz, C., Sciare, J., Teinilä, K., Vermeylen, R., Vicente, A., and Zimmermann, R.: An intercomparison study of analytical methods used for quantification of levoglucosan in ambient aerosol filter samples, Atmos. Meas. Tech., 8, 125–147, 2015, doi:10.5194/amt-8-125-2015.

Supplementary Figures

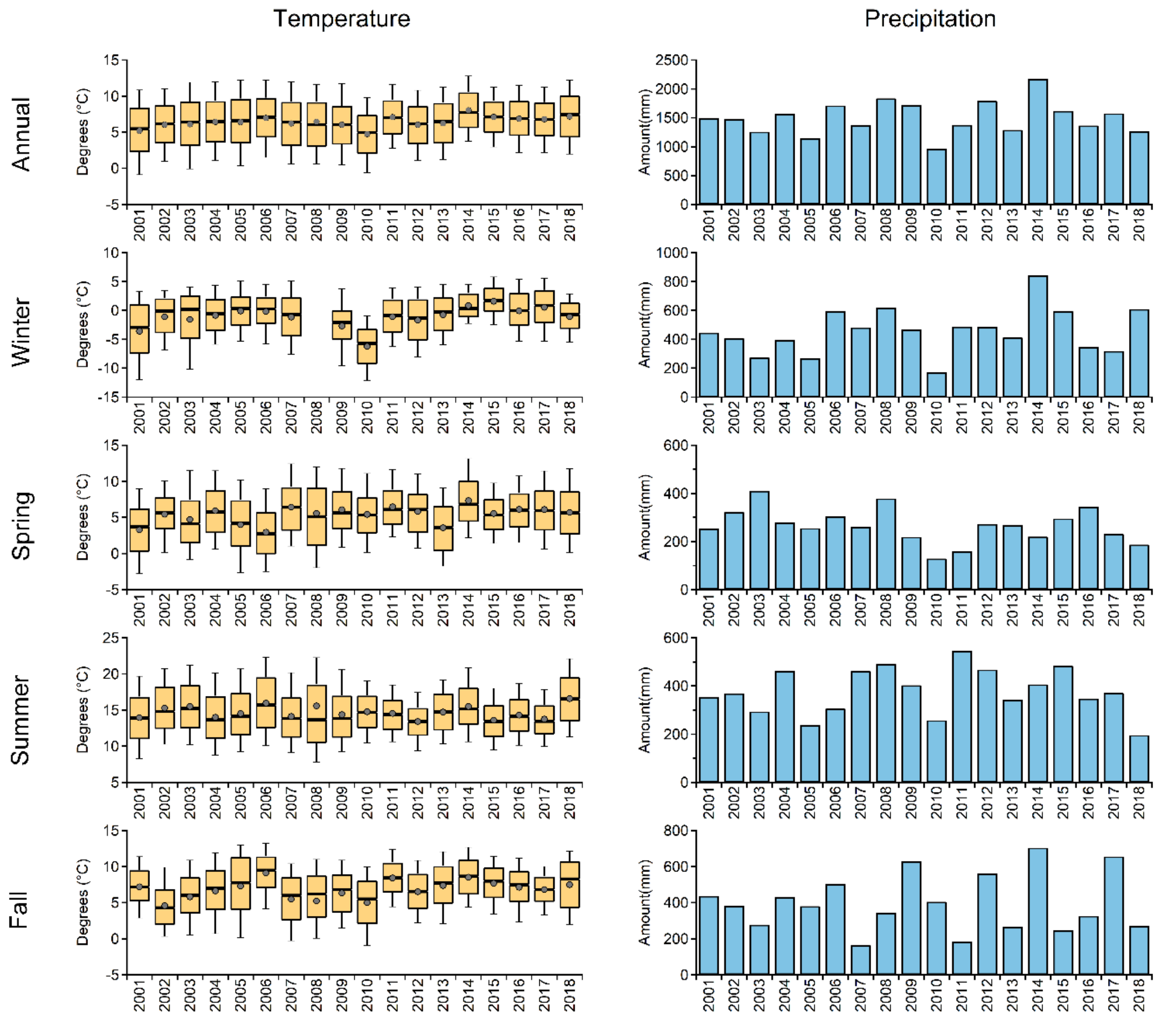

Figure S 1: Annual and seasonal ambient mean (point), 10th to 25th percentile (bar), 50th percentile (line), 75th to 90th percentile (whisker) temperature (left panel) and precipitation (right panel) at the Birkenes Observatory, 2001–2018.

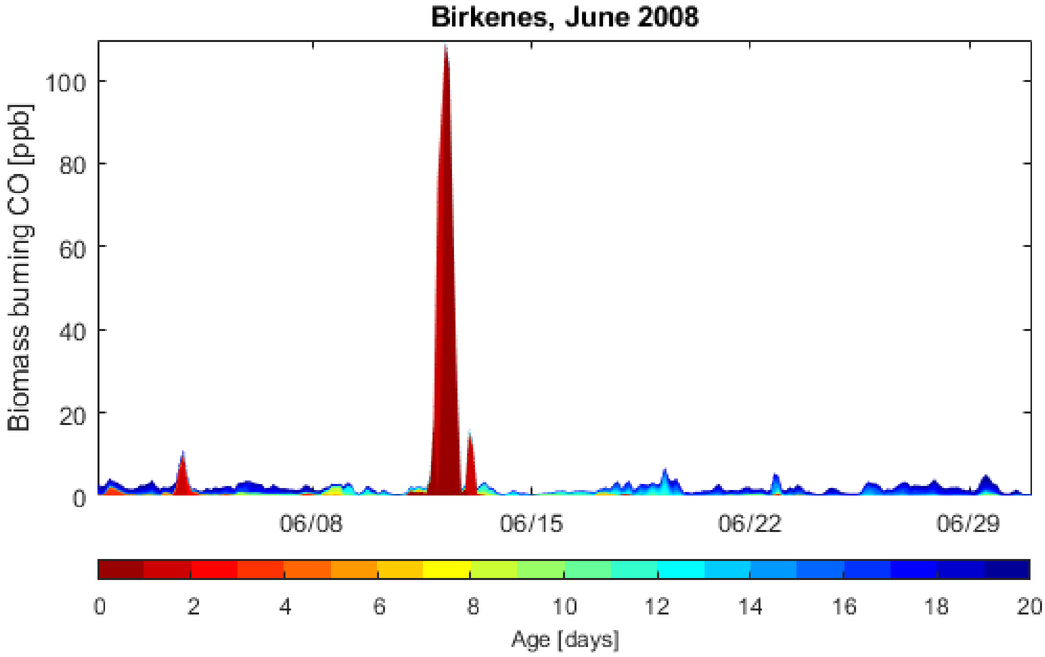

Figure S 2: Age spectra for June 2008 for the CO tracer originating from wildfires calculated for the Birkenes Observatory. We ran a 20 days FLEXPART simulation backwards in time, releasing 40 000 particles for the Birkenes Observatory on a 3-hourly basis, using ECMWF meteorology. With daily MODIS information of burned area we constructed a CO emission inventory, which we combined with the model simulation. With this approach we achieved a time series of CO from wildfires with a 3-hourly time resolution. Additionally, we split the modeled CO concentrations by age. The spectrum goes from 1 to 20 days after release according to the color bar (Figure S 2). This approach is described in more detail in Stohl et al. (2007). For most of June 2008, concentrations of a few ppb were calculated for the Birkenes Observatory, except for 11–12 of June (100 ppb). The age of the airmasses were only 1 day, which means that the CO was released on a location less than 24 hours before it reached the site.

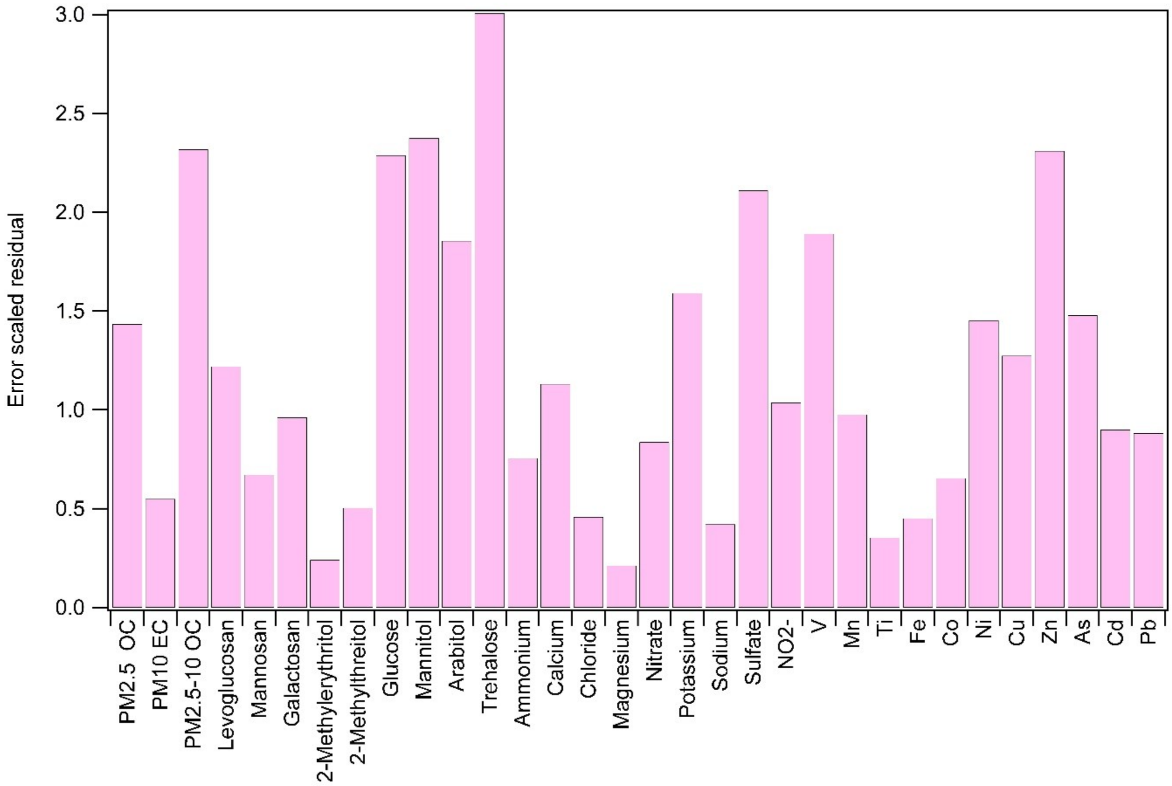

Figure S 3: Average error scaled residuals for each of the variables in the PMF solution presented in this paper

Supplementary Tables

Table S 1: Species quantification ion, molecular weight and formula, and internal/recovery and quantification standards used for their identification and quantification.

Species	Quantitation ion M-H(+)	Molecular weight	Molecular formula	Internal/ Recovery standard	Quantification standard
Monosaccharide anhydrides					
Galactosan	161.046	162.141	$C_6H_{10}O_5$	$^{13}C_6$-Galactosan (CIL; 98%; Andover, MA)	Galactosan (Sigma; purity not given; Product of England)
Mannosan	161.046	162.141	$C_6H_{10}O_5$	$^{13}C_6$-Levoglucosan[1] $^{13}C_6$-Galactosan[1]	Mannosan (Sigma; Approx 98%; Product of England)
Levoglucosan	161.046	162.141	$C_6H_{10}O_5$	$^{13}C_6$-Levoglucosan (CIL; 98%; city not given)	Levoglucosan (Aldrich; 99%; Product of Switzerland)
Sugar-alcohols					
Mannitol	181.072	182.172	$C_6H_{14}O_6$	$^{13}C_6$-Mannitol (Omnicron Biochemicals Inc; 99.70%; South Bend, Indiana)	Mannitol (ICN Biochemicals; ACS reagent grade; Aurora, Ohio)
Arabitol	151.061	152.15	$C_5H_{12}O_6$	$^{13}C_5$-Arabitol (Omnicron Biochemicals Inc; 99.60%; South Bend, Indiana)	Arabitol (ICN Biochemicals; purity not given; Aurora, Ohio)
2-methyltetrols					
2-Methylerythritol	135.066	136.147	$C_5H_{12}O_4$	$^{13}C_6$-Galactosan (CIL; 98%; Andover, MA)	2-Methylterythritol, Produced at UNC[2]
2-Methylthreitol	135.066	136.147	$C_5H_{12}O_4$	$^{13}C_6$-Galactosan (Brand; purity; city)	2-Methylthreitol, Produced at UNC[2]
Dimeric sugars					
Trehalose	341.109	342.296	$C_{12}H_{22}O_{11}$	$^{13}C_{12}$-Trehaose (Omnicron Biochemicals Inc; 99.70%; South Bend, Indiana)	Trehalose (Fluka; <99.5%; Packed in Switzerland)
Monomeric sugars					
Glucose	179.0561	180.16	$C_6H_{12}O_6$	$^{13}C_1$-Glucose (CIL; 99%; Andover, MA)	Glucose (Sigma; purity not given; city not given)

1.C-labelled mannosan is not commersially available, hence we used the average of $^{13}C_6$-Levoglucosan $^{13}C_6$-Galactosan to calculate the recovery of mannosan.

2.Standard produced by University of North Carolina (UNC)

Table S 2: Settings used for absorption coefficient PMF analysis.

Parameter	Setting
Data matrix dimensions i×j	5240×7
Missing data treatment	Rows removed
Number of factors	2
Factor constraints	None
Robust mode setting	4
Seed	Random
Bootstrap replacement runs	2000
Block size	24
Repeat runs (per bootstrap)	5

Table S 3: Miscellaneous settings of PMF analysis.

Parameter	Setting
Data matrix dimensions i×j	151×34
Missing data and below detection limit data	Replaced with geometric mean concentration
Missing data error estimate	Replaced with 4 × geometric mean concentration
Missing data error estimate	5/6 × limit of detection
Number of factors	7
Factor contsraints	None
Robust mode setting	4
Seed	Random
Bootstrap replacement runs	5000
Block size	1 row
Repeat runs (per bootstrap)	5

Table S 4: Contribution weighted relative profiles for PMF–derived factors (%).

	Mineral Dust (MIN)	Traffic/Industry (TRA/IND)	Biogenic Secondary Organic Aerosol ($BSOA_{SRT}$)	Primary Biological Aerosol Particle (PBAP)	Sea salt aerosol (SS)	Biomass burning (BB)	Ammonium Nitrate (NH_4NO_3)
$PM_{2.5}$ OC	31.3	9.7	9.1	15.6	0.9	16.7	16.6
PM_{10} EC	12.8	50.0	0.0	2.6	0.0	21.2	13.4
$PM_{10-2.5}$ OC	12.6	3.5	12.5	53.0	0.1	6.3	12.0
Levoglucosan	0.2	0.0	1.5	0.5	0.0	97.8	0.0
Mannosan	0.0	0.5	1.5	1.5	0.0	95.6	0.9
Galactosan	0.0	3.5	0.0	0.0	1.1	95.5	0.0
2-methylerythritol	0.5	0.7	95.9	1.8	0.0	0.4	0.7
2-methylthreitol	0.6	1.3	91.5	3.2	0.7	1.5	1.2
Glucose	1.0	0.6	6.5	81.6	2.0	5.2	3.1
Mannitol	0.1	0.3	6.1	91.3	1.7	0.0	0.5
Arabitol	0.0	0.0	8.6	89.5	1.3	0.5	0.0
Trehalose	0.5	0.0	3.3	93.5	1.1	0.7	0.9
Ammonium	2.1	13.9	4.8	0.0	1.5	1.0	76.7
Calcium	39.0	6.0	7.7	3.9	34.9	1.0	7.6
Chloride	0.0	0.0	0.0	0.0	96.2	0.2	3.5
Magnesium	5.8	2.7	3.9	1.8	79.0	0.6	6.2
Nitrate	0.8	3.6	5.7	3.4	17.1	1.7	67.8
Potassium	3.6	12.7	4.6	8.3	28.4	10.4	32.0
Sodium	2.2	5.1	2.7	0.0	86.8	0.3	3.0
Sulfate	3.9	19.6	17.2	3.3	17.4	3.4	35.2
NO_2^-	7.2	15.0	4.6	4.6	20.0	19.0	29.7
V	14.1	70.1	10.1	0.0	0.0	0.0	5.8
Mn	51.9	38.6	0.6	5.7	2.4	0.8	0.0
Ti	93.4	0.5	0.6	0.0	3.7	1.8	0.0
Fe	74.5	18.4	0.0	3.2	0.7	1.0	2.1
Co	42.6	42.1	1.3	3.3	5.0	2.4	3.4
Ni	17.1	68.6	3.0	4.5	1.7	2.1	2.9

	Mineral Dust (MIN)	**Traffic/Industry (TRA/IND)**	**Biogenic Secondary Organic Aerosol ($BSOA_{SRT}$)**	**Primary Biological Aerosol Particle (PBAP)**	**Sea salt aerosol (SS)**	**Biomass burning (BB)**	**Ammonium Nitrate (NH_4NO_3)**
Cu	19.9	61.9	3.3	3.7	5.7	1.3	4.2
Zn	4.3	81.5	1.4	0.6	0.0	5.8	6.4
As	3.2	78.4	1.7	6.2	0.0	4.8	5.7
Cd	5.4	80.5	0.1	2.3	1.6	6.4	3.8
Pb	4.5	83.9	0.8	0.0	1.5	2.8	6.4

Table S 5: Annual and seasonal mean concentrations of EC and OC in PM_{10}, $PM_{2.5}$ and $PM_{10-2.5}$ at Birkenes for 2001–2018 (Unit: $\mu g\ C\ m^{-3}$).

	PM10				PM10-2.5		PM2.5			
	OC	Capture	EC	Capture	OC	Capture	OC	Capture	EC	Capture
2001	***0.96***	***56***	***0.14***	***56***	***0.08***	***45***	***0.93***	***56***	***0.15***	***56***
DJF	0.60	59	0.12	59	NA	34	0.64	59	0.12	59
MAM	0.98	92	0.16	92	0.03	73	1.00	92	0.18	92
JJA	2.34	26	0.16	26	0.24	26	2.1	26	0.20	26
SON	0.58	48	0.10	48	0.09	48	0.49	48	0.11	48
2002	***1.01***	***85***	***0.14***	***85***	***0.190***	***80***	***0.89***	***91***	***0.12***	***91***
DJF	0.53	95	0.12	95	0.05	88	0.49	95	0.12	95
MAM	1.30	92	0.17	92	0.12	92	1.19	92	0.14	92
JJA	1.77	68	0.20	68	0.48	68	1.4	91	0.14	91
SON	0.59	86	0.10	86	0.16	73	0.49	85	0.09	85
2003	***1.01***	***82***	***0.10***	***82***	***0.23***	***77***	***0.81***	***81***	***0.11***	***81***
DJF	0.83	85	0.11	85	0.06	76	0.84	85	0.12	85
MAM	1.13	86	0.13	86	0.21	76	1.02	86	0.15	86
JJA	1.26	85	0.08	85	0.44	85	0.82	85	0.09	85
SON	0.75	70	0.09	70	0.22	70	0.53	70	0.09	70
2004	***0.82***	***85***	***0.10***	***85***	***0.27***	***81***	***0.57***	***84***	***0.09***	***84***
DJF	0.57	86	0.08	86	0.09	86	0.48	86	0.08	86
MAM	1.13	86	0.12	86	0.28	73	0.79	86	0.12	86
JJA	0.99	79	0.10	79	0.38	79	0.61	79	0.08	79
SON	0.71	86	0.08	86	0.32	86	0.39	86	0.08	80
2005	***0.85***	***79***	***0.14***	***79***	***0.29***	***75***	***0.60***	***80***	***0.12***	***80***
DJF	0.46	64	0.10	64	0.06	51	0.53	71	0.11	71
MAM	0.78	85	0.13	86	0.15	85	0.63	85	0.12	85
JJA	0.92	86	0.09	85	0.33	86	0.59	86	0.08	86
SON	1.16	79	0.25	79	0.53	79	0.62	79	0.16	79
2006	***1.07***	***78***	***0.13***	***78***	***0.33***	***75***	***0.77***	***78***	***0.13***	***78***
DJF	0.79	86	0.12	86	0.08	79	0.71	86	0.17	86
MAM	0.95	85	0.08	85	0.16	78	0.82	85	0.14	85
JJA	1.43	57	0.12	57	0.48	57	0.96	57	0.10	57
SON	1.24	86	0.19	86	0.60	86	0.64	86	0.11	86
2007	***0.82***	***79***	***0.15***	***77***	***0.21***	***77***	***0.61***	***77***	***0.13***	***77***
DJF	0.58	58	0.17	58	0.08	58	0.50	58	0.17	58
MAM	0.99	86	0.18	85	0.17	86	0.82	86	0.15	86
JJA	1.03	86	0.13	86	0.39	79	0.66	79	0.10	79
SON	0.60	86	0.13	79	0.18	86	0.41	86	0.10	86
2008	***0.75***	***87***	***0.09***	***84***	***0.24***	***75***	***0.53***	***88***	***0.08***	***88***
DJF	0.44	90	0.08	83	0.07	82	0.38	90	0.09	84
MAM	0.79	86	0.11	92	0.20	79	0.61	86	0.10	86
JJA	1.27	86	0.08	86	0.46	86	0.81	86	0.06	86
SON	0.51	90	0.09	82	0.23	82	0.32	90	0.08	97
2009	***0.79***	***98***	***0.10***	***98***	***0.23***	***77***	***0.58***	***96***	***0.09***	***96***
DJF	0.56	100	0.12	100	0.06	69	0.47	92	0.11	92
MAM	0.81	92	0.11	85	0.11	85	0.74	92	0.10	92
JJA	1.1	100	0.09	100	0.40	100	0.71	100	0.07	100
SON	0.68	100	0.09	100	0.28	100	0.40	100	0.07	100
2010	***0.90***	***94***	***0.11***	***94***	***0.24***	***79***	***0.67***	***96***	***0.10***	***96***
DJF	0.95	92	0.14	92	0.09	40	0.86	92	0.16	92
MAM	0.82	85	0.09	85	0.18	82	0.61	100	0.08	100
JJA	1.02	100	0.09	100	0.34	100	0.68	100	0.07	100
SON	0.79	100	0.11	100	0.24	100	0.51	92	0.09	92
2011	***0.92***	***98***	***0.11***	***92***	***0.26***	***94***	***0.68***	***98***	***0.11***	***96***
DJF	0.60	100	0.11	100	0.09	92	0.51	92	0.11	100
MAM	0.99	93	0.10	70	0.27	93	0.73	100	0.10	85
JJA	1.07	100	0.07	100	0.37	100	0.69	100	0.07	100
SON	1.04	100	0.17	100	0.30	92	0.77	100	0.16	100
2012	***0.56***	***89***	***0.08***	***86***	***0.10***	***79***	***0.50***	***90***	***0.08***	***90***

	PM_{10}				$PM_{10-2.5}$		$PM_{2.5}$			
	OC	**Capture**	**EC**	**Capture**	**OC**	**Capture**	**OC**	**Capture**	**EC**	**Capture**
DJF	0.52	100	0.09	100	0.04	84	0.49	100	0.09	100
MAM	0.58	85	0.09	85	0.03	70	0.63	70	0.11	70
JJA	0.78	70	0.07	70	0.18	70	0.59	100	0.07	100
SON	0.56	100	0.07	92	0.14	92	0.30	92	0.07	92
2013	***0.76***	***92***	***0.09***	***96***	***0.21***	***90***	***0.57***	***98***	***0.08***	***96***
DJF	0.49	92	0.10	92	0.05	68	0.47	91	0.09	91
MAM	0.79	100	0.10	100	0.15	100	0.63	100	0.09	100
JJA	1.16	100	0.07	92	0.37	100	0.79	100	0.07	92
SON	0.58	100	0.07	100	0.22	92	0.39	100	0.07	100
2014	***0.91***	***98***	***0.09***	***100***	***0.29***	***94***	***0.65***	***96***	***0.08***	***96***
DJF	0.61	100	0.10	100	0.08	76	0.59	84	0.11	84
MAM	0.91	100	0.10	100	0.23	100	0.69	100	0.09	100
JJA	1.10	100	0.05	100	0.35	100	0.75	100	0.05	100
SON	1.20	100	0.10	100	0.47	100	0.55	100	0.09	100
2015	***0.72***	***98***	***0.09***	***98***	***0.19***	***85***	***0.52***	***88***	***0.08***	***88***
DJF	0.44	100	0.06	100	0.11	100	0.34	100	0.06	100
MAM	0.59	92	0.10	92	0.11	79	0.50	92	0.08	92
JJA	1.01	100	0.09	100	0.35	63	0.66	63	0.08	63
SON	0.83	100	0.10	100	0.22	99	0.62	99	0.10	99
2016	***0.73***	***100***	***0.06***	***100***	***0.21***	***95***	***0.54***	***100***	***0.06***	***100***
DJF	0.44	100	0.07	100	0.07	86	0.37	100	0.06	100
MAM	0.83	100	0.07	100	0.21	92	0.64	100	0.07	100
JJA	0.98	100	0.04	100	0.33	100	0.65	100	0.05	100
SON	0.68	100	0.07	100	0.20	100	0.48	100	0.07	100
2017	***0.72***	***94***	***0.05***	***94***	***0.25***	***79***	***0.52***	***94***	***0.05***	***94***
DJF	0.57	100	0.07	100	0.11	63	0.53	100	0.07	100
MAM	0.65	92	0.05	92	0.14	84	0.52	92	0.05	92
JJA	0.92	86	0.03	86	0.34	86	0.58	86	0.04	86
SON	0.77	100	0.06	100	0.38	83	0.47	100	0.05	100
2018	***0.96***	***100***	***0.08***	***100***	***0.26***	***90***	***0.73***	***100***	***0.07***	***100***
DJF	0.49	100	0.07	100	0.08	77	0.45	100	0.07	100
MAM	1.32	100	0.11	100	0.28	92	1.06	100	0.10	100
JJA	1.20	100	0.05	100	0.32	100	0.90	100	0.05	100
SON	0.81	100	0.08	100	0.31	100	0.50	100	0.07	100

Notation: Red numbers indicate annual or seasonal means based on < 50% data capture.

Table S 6: R^2-values for OC versus EC as a function of size fraction and season.

	Winter	Spring	Summer	Fall
PM_{10}	0.66	0.58	0.51	0.64
$PM_{2.5}$	0.75	0.69	0.58	0.76

Table S 7: Annual mean (±SD) relative chemical composition for the period 2001–2018. Unit (%)[1]

	OM/PM_{10}	EC/PM_{10}	SO_4^{2-}/PM_{10}	NO_3^-/PM_{10}	NH_4^+/PM_{10}	SS/PM_{10}	$OM/PM_{2.5}$	$EC/PM_{2.5}$	$OM/PM_{10-2.5}$
2001	31±4	2.7±0.4	21	11	6	11	38±5	3.6±0.5	8.9±1.8[1)]
2002	26±4	2.1±0.3	20	14	8	10	30±4	2.3±0.3	16±3
2003	29±4	1.6±0.2	23	12	6	11	32±5	2.5±0.4	18±4
2004	27±4	1.9±0.3	19	15	7	14	32±5	2.9±0.4	21±4
2005	25±4	2.4±0.3	20	16	8	13	29±4	3.3±0.5	21±4
2006	26±4	1.8±0.3	20	17	5	12	31±4	3.0±0.4	18±4
2007	27±4	2.9±0.4	15	10	4	14	35±5	4.3±0.6	16±3
2008	25±4	1.7±0.2	14	12	3	18	36±5	3.1±0.4	17±3
2009	26±4	3.7±1.9	15	13	4	13	31±4	2.8±0.4	19±4
2010	34±5	2.4±0.3	17	13	5	11	37±5	3.2±0.5	21±4
2011	25±4	1.7±0.2	14	17	6	16	32±4	3.0±0.4	15±3
2012	22±3	1.8±0.3	17	28	7	17	33±5	3.0±0.4	10±2
2013	29±4	2.0±0.3	15	19	6	23	37±5	3.0±0.4	18±4
2014	28±4	1.6±0.2	18	21	7	20	36±5	2.6±0.4	20±4
2015	26±4	1.9±0.3	16	22	6	28	36±5	3.3±0.5	20±3
2016	32±5	1.5±0.2	14	23	7	23	41±6	2.6±0.4	21±4
2017	38±5	1.5±0.2	19	14	5	27	49±7	2.8±0.4	28±6
2018	34±5	1.6±0.2	14	15	6	19	46±7	2.6±0.4	20±4

[1] 1) Data capture below 50%.
2) Notation: Conversion factors applied OM = OC x 1.9; EC = EC x 1.1

Table S 8: Mean (±SD) relative chemical composition of the 3 weekly samples with the highest PM mass concentration (PM_{MAX}) per year for the period 2001–2018.[2]

	$PM_{10\,MAX}$		OM	EC	SO_4^{2-}	NO_3^-	NH_4^+	SS	$PM_{2.5\,MAX}$		OM	EC
	$\mu g\ m^{-3}$	Season[1)]	%	%	%	%	%	%	$\mu g\ m^{-3}$	Season[1)]	%	%
2001	12.4±1.6	234	43±16	3±1	14±10	4±3	4±3	3±3	12.2±2.4	234	50±10	5±2
2002	23.8±3.6	223	26±11	1.8±0.7	14±9	13±14	8±4	2±2	18.8±2.9	223	29±12	1.7±0.5
2003	17.9±2.7	222	16±3	1.3±0.4	17±3	18±8	11±2	8±3	12.0±1.9	222	19±3	1.6±0.3
2004	17.0±6.8	222	23±9	1.5±0.4	21±3	11±10	8±4	14±18	11.6±6.5	222	27±9	2.4±0.8
2005	16.9±2.8	244	26±6	3.4±1.6	15±3	20±3	2±0	5±3	12.4±3.1	224	27±10	2.9±0.4
2006	26.5±3.0	144	23±8	4.1±1.6	19±7	17±4	8±2	7±5	15.5±0.9	124	30±10	2.3±0.7
2007	13.8±3.5	223	40±2	4.2±1.5	12±0	6±2	4±1	1±0	10.7±3.4	223	48±2	4.1±1.5
2008	12.5±3.0	222	12±5	1.5±0.5	12±3	20±7	5±3	15±15	7.0±2.7	223	16±3	1.9±0.6
2009	14.8±5.7	222	21±1	1.8±0.0	12±5	13±9	5±3	3±2	10.6±4.1	122	28±3	2.5±0.5
2010	12.0±2.4	344	21±6	1.9±0.6	14±3	13±2	3±1	23±11	10.7±3.7	144	42±9	5.0±0.6
2011	16.7±1.2	224	23±13	2.0±1.3	23±2	17±4	12±0	2±1	12.1±1.5	224	27±13	3.0±1.9
2012	11.9±1.7	122	29±21	3.9±3.4	10±9	24±25	3±2	1±0	7.2±1.4	123	30±26	3.0±2.7
2013	9.4±0.6	222	12±4	1.4±0.5	9±2	7±2	8±0	13±5	5.7±0.6	223	30±9	2.6±1.0
2014	17.7±3.3	224	18±8	1.5±0.2	15±5	25±6	10±1	14±8	8.1±0.9	122	21±6	2.5±0.5
2015	12.0±4.0	122	21±10	2.2±1.3	12±7	23±10	11±2	12±12	6.9±1.7	122	31±20	3.3±2.0
2016	9.2.±0.2	223	30±22	1.3±0.3	6±5	18±17	7±7	6±1	6.7±1.5	223	37±25	1.9±0.3
2017	9.8.±2.7	114	33±8	2.3±1.1	19±3	14±7	7±1	13±13	6.3±2.0	112	29±8	2.7±0.3
2018	12.8.±3.1	124	32±24	1.3±0.5	11±3	20±15	8±5	5±1	9.0±1.0	144	21±11	1.7±1.2

[2] 1 = DJF; 2 = MAM; 3 = JJA; 4 = SON

Table S 9: Annual and seasonal mean concentrations of TC in PM_{10}, $PM_{2.5}$ and $PM_{10-2.5}$ at Birkenes for 2001–2018 (Unit: *$\mu g\ C\ m^{-3}$*).

	PM_{10} TC	Capture	$PM_{10-2.5}$ TC	Capture	$PM_{2.5}$ TC	Capture
2001	***1.09***	***63***	***0.07***	***48***	***1.08***	***63***
DJF	0.72	59	0	34	0.75	59
MAM	1.14	92	0.02	65	1.19	92
JJA	2.50	26	0.20	26	2.30	26
SON	0.68	48	0.08	48	0.60	48
2002	***1.15***	***85***	***0.21***	***80***	***1.01***	***91***
DJF	0.65	95	0.05	88	0.60	95
MAM	1.47	92	0.14	92	1.33	92
JJA	1.96	68	0.53	68	1.50	91
SON	0.68	86	0.18	73	0.59	86
2003	***1,12***	***82***	***0,23***	***78***	***0,93***	***82***
DJF	0.94	85	0.05	82	0.95	85
MAM	1.26	86	0.20	76	1.16	86
JJA	1.34	85	0.43	85	0.91	85
SON	0.84	70	0.22	70	0.62	70
2004	***0.91***	***84***	***0.28***	***79***	***0.65***	***84***
DJF	0.65	86	0.09	86	0.56	86
MAM	1.13	86	0.32	66	0.91	86
JJA	1.09	79	0.41	79	0.68	79
SON	0.79	86	0.33	86	0.47	86
2005	***0.99***	***79***	***0.32***	***75***	***0.71***	***80***
DJF	0.56	64	0.06	51	0.64	71
MAM	0.91	85	0.16	85	0.75	85
JJA	1.01	86	0.34	86	0.67	86
SON	1.41	79	0.62	79	0.79	79
2006	***1.20***	***78***	***0.35***	***70***	***0.90***	***78***
DJF	0.91	86	0.08	66	0.88	86
MAM	1.03	85	0.10	72	0.96	85
JJA	1.55	57	0.49	57	1.06	57
SON	1.43	86	0.68	86	0.75	86
2007	***0.99***	***77***	***0.24***	***76***	***0.74***	***77***
DJF	0.76	58	0.09	58	0.67	58
MAM	1.17	86	0.20	86	0.97	86
JJA	1.16	86	0.41	79	0.77	79
SON	0.76	79	0.21	79	0.52	86
2008	***0.85***	***84***	***0.25***	***81***	***0.60***	***86***
DJF	0.47	84	0.05	76	0.43	84
MAM	0.90	86	0.21	79	0.71	86
JJA	1.35	86	0.47	86	0.87	86
SON	0.65	82	0.24	82	0.39	90
2009	***0.89***	***98***	***0.23***	***92***	***0.67***	***96***
DJF	0.68	100	0.05	84	0.58	92
MAM	0.92	92	0.12	85	0.85	92
JJA	1.19	100	0.41	100	0.78	100
SON	0.76	100	0.29	100	0.47	100
2010	***1.00***	***94***	***0.21***	***87***	***0.77***	***96***
DJF	1.09	92	0.06	69	1.03	92
MAM	0.91	85	0.17	85	0.69	100
JJA	1.11	100	0.36	100	0.75	100
SON	0.90	100	0.26	92	0.61	92
2011	***0.99***	***98***	***0.25***	***92***	***0.80***	***100***
DJF	0.71	100	0.09	92	0.64	100
MAM	0.88	92	0.20	85	0.84	100
JJA	1.13	100	0.37	100	0.76	100
SON	1.21	100	0.32	92	0.93	100
2012	***0.64***	***89***	***0.10***	***79***	***0.58***	***92***

	PM_{10} TC	Capture	$PM_{10-2.5}$ TC	Capture	$PM_{2.5}$ TC	Capture
DJF	0.61	100	0.03	92	0.58	100
MAM	0.67	85	0	68	0.73	77
JJA	0.85	70	0.25	56	0.66	100
SON	0.51	100	0.14	92	0.37	92
2013	***0.84***	***98***	***0.21***	***92***	***0.65***	***98***
DJF	0.59	92	0.04	76	0.56	91
MAM	0.89	100	0.17	100	0.72	100
JJA	1.22	100	0.37	100	0.86	100
SON	0.66	100	0.23	92	0.46	100
2014	***1.00***	***100***	***0.30***	***94***	***0.73***	***96***
DJF	0.71	100	0.07	76	0.70	84
MAM	1.02	100	0.24	100	0.78	100
JJA	1.16	100	0.35	100	0.80	100
SON	1.12	100	0.48	100	0.64	100
2015	**0.81**	***98***	***0.19***	***88***	***0.60***	***88***
DJF	0.50	100	0.11	100	0.39	100
MAM	0.70	92	0.10	92	0.60	92
JJA	1.10	100	0.36	63	0.74	63
SON	0.94	100	0.23	96	0.71	96
2016	***0.80***	***100***	***0.21***	***94***	***0.6***	***100***
DJF	0.51	100	0.08	82	0.43	100
MAM	0.90	100	0.22	92	0.71	100
JJA	1.02	100	0.32	100	0.70	100
SON	0.76	100	0.21	100	0.55	100
2017	***0.78***	***94***	***0.26***	***78***	***0.58***	***94***
DJF	0.63	100	0.11	59	0.60	100
MAM	0.70	92	0.14	84	0.58	92
JJA	0.95	86	0.34	86	0.61	86
SON	0.84	100	0.40	83	0.51	100
2018	***1.03***	***100***	***0.26***	***90***	***0.8***	***100***
DJF	0.56	100	0.08	77	0.52	100
MAM	1.43	100	0.30	92	1.06	100
JJA	1.25	100	0.32	92	0.95	100
SON	0.88	100	0.32	100	0.56	100

Notation: Red numbers indicate annual or seasonal means based on < 50% data capture.

Table S 10: Annual and seasonal mean mass concentrations of PM_{10}, $PM_{2.5}$ and $PM_{10-2.5}$ at Birkenes for 2001–2018 (Unit: *$\mu g\ m^{-3}$*).

	PM_{10}	Capture	$PM_{2.5}$	Capture	$PM_{10-2.5}$	Capture
2001	***5.8***	***56***	***4.6***	***58***	***1.7***	***54***
DJF	4.5	59	3.2	59	1.3	59
MAM	6.6	92	5.5	100	1.8	92
JJA	7.9	26	7.3	26	1.3	19
SON	4.9	48	2.9	48	1.9	48
2002	***7.5***	***83***	***5.7***	***91***	***2.2***	***80***
DJF	5.6	88	3.8	95	1.8	88
MAM	11.0	92	8.5	92	2.4	92
JJA	10.0	68	7.3	95	2.9	68
SON	3.9	86	2.8	86	1.5	73
2003	***6.7***	***78***	***4.8***	***82***	***2.4***	***74***
DJF	5.9	76	4.4	85	2.2	76
MAM	9.3	82	6.7	86	3.4	76
JJA	5.9	85	4.4	81	1.7	79
SON	5.4	70	3.5	70	2.3	64
2004	***5.7***	***84***	***3.4***	***84***	***2.4***	***83***
DJF	4.5	86	2.8	86	1.7	86
MAM	8.2	86	5.4	85	3.1	79
JJA	5.7	79	3.3	79	2.4	79
SON	4.3	86	2.0	86	2.3	86
2005	***6.5***	***79***	***4.0***	***80***	***2.6***	***75***
DJF	5.2	64	3.1	71	2.8	51
MAM	6.9	85	4.9	85	1.9	85
JJA	5.5	86	3.4	86	2.1	86
SON	8.0	79	4.4	79	3.6	79
2006	***7.8***	***78***	***4.7***	***77***	***3.4***	***73***
DJF	7.4	86	4.5	79	3.0	79
MAM	6.2	85	4.6	86	2.1	72
JJA	8.3	57	5.4	57	3.0	57
SON	9.5	86	4.5	86	5.0	86
2007	***5.8***	***72***	***3.3***	***74***	***2.5***	***72***
DJF	4.2	38	2.0	38	2.2	38
MAM	7.5	86	4.4	86	3.1	86
JJA	6.1	79	3.5	86	2.5	79
SON	4.4	86	2.4	86	2.0	86
2008	***5.7***	***77***	***2.8***	***86***	***2.7***	***75***
DJF	5.1	84	2.5	90	2.8	84
MAM	7.1	79	4.1	73	2.7	73
JJA	6.1	86	3.1	86	2.9	86
SON	4.0	58	1.9	97	2.1	58
2009	***5.8***	***85***	***3.6***	***94***	***2.3***	***76***
DJF	4.4	96	3	92	1.4	88
MAM	9.4	74	5.3	100	3.4	74
JJA	6.1	71	3.8	92	2.2	63
SON	4.3	99	2.2	92	2.3	83

	PM_{10}	Capture	$PM_{2.5}$	Capture	$PM_{10-2.5}$	Capture
2010	***5.1***	***88***	***3.4***	***94***	***2.2***	***77***
DJF	3.8	100	3.4	87	0.55	64
MAM	5.4	71	3	98	2.3	68
JJA	6.7	90	3.7	100	3.1	91
SON	4.8	92	3.5	92	2.5	85
2011	***7.0***	***98***	***4.1***	***100***	***3.2***	***96***
DJF	5.6	100	3.1	100	2.5	100
MAM	8.2	93	5.5	100	3.9	85
JJA	5.2	100	3.5	100	1.7	100
SON	9.0	100	4.4	100	4.6	100
2012	***4.9***	***89***	***2.9***	***92***	***2.0***	***85***
DJF	4.4	100	2.7	100	1.7	99
MAM	6.7	85	3.2	100	3.3	70
JJA	4.6	70	3.8	70	1.4	70
SON	4.0	100	2.0	100	2.0	100
2013	***4.9***	***92***	***2.9***	***86***	***2.2***	***84***
DJF	3.8	69	2.6	44	1.7	44
MAM	6.4	100	3.7	100	2.8	100
JJA	5.4	100	3.4	100	2.0	100
SON	3.6	100	1.8	100	2.0	92
2014	***6.1***	***98***	***3.4***	***96***	***2.7***	***94***
DJF	5.7	100	3.5	84	2.4	84
MAM	7.2	92	3.7	100	3.3	92
JJA	5.2	100	3.2	100	2.0	100
SON	6.3	100	3.3	100	3.0	100
2015	***5.3***	***98***	***2.7***	***88***	***2.5***	***88***
DJF	5.5	100	2.5	100	31	100
MAM	5.2	100	2.8	100	2.5	100
JJA	5.5	92	2.9	63	1.9	63
SON	5.0	100	2.8	99	2.4	99
2016	**4.3**	**100**	**2.5**	**100**	**1.9**	**100**
DJF	4.1	100	2.1	100	2.0	100
MAM	4.8	100	3.1	100	1.7	100
JJA	4.3	100	2.6	100	1.7	100
SON	4.1	100	2.1	100	2.1	100
2017	**3.8**	**90**	**2.0**	**94**	**1.7**	**90**
DJF	3.7	100	2.2	100	1.4	100
MAM	3.8	92	2.3	92	1.5	92
JJA	3.9	86	2.1	86	1.8	86
SON	3.8	85	1.4	100	2.4	85
2018	**5.4**	**100**	**3.0**	**98**	**2.5**	**98**
DJF	3.8	100	2.4	92	1.4	92
MAM	6.5	100	4.2	100	2.3	100
JJA	5.4	100	3.1	100	2.3	100
SON	6.2	100	2.2	100	3.9	100

Red numbers indicate annual or seasonal means based on < 50% data capture.

Table S 11: Sen slope of annual means and corresponding confidence intervals for significant slopes (*p=0.05*), as well as change in annual mean presented as percentage change per year and as percentage change for the period 2001–2018. Non-significant values in red.

	Slope (% yr^{-1})	CI-1	CI-2	Change 2001-2018 (%)
PM_{10}	-2.2	-3.7	-0.7	-38
$PM_{2.5}$	-4.0	-5.7	-2.2	-69
$PM_{10-2.5}$	-0.1	-2.2	1.4	-2.4
OC in PM_{10}	0	-1.4	0.9	0
OC in $PM_{2.5}$	-0.8	-2.8	0.7	-13
OC in $PM_{10-2.5}$	0.8	-1.7	3.4	13
EC in PM_{10}	-3.9	-5.8	-1.9	-66
EC in $PM_{2.5}$	-4.2	-6.2	-2.6	-71
TC in PM_{10}	-1.1	-2.0	0.0	-19
TC in $PM_{2.5}$	-1.5	-3.5	0.0	-26
TC in $PM_{10-2.5}$	0.0	-2.4	1.9	0
SO_4^{2-}	-3.8	-6.1	-1.8	-65
NO_3^-	0.8	-2.5	4.3	14
NH_4^+	-2.7	-5.8	0.5	-47
SS	2.2	0.6	4.5	38
Levoglucosan[1)]	-2.8	-8.8	-0.2	-28

Notation: Trends for levoglucosan are calculated for the period 2008–2018.

Table S 12: Sen slope of seasonal means in % yr^{-1} and corresponding confidence intervals for significant slopes (*p=0.05*) for 2001–2018. Non-significant values in red.

	DJF			MAM			JJA			SON		
	Slope (% yr^{-1})	CI-1	CI-2	Slope (% yr^{-1})	CI-1	CI-2	Slope (% yr^{-1})	CI-1	CI-2	Slope (% yr^{-1})	CI-1	CI-2
PM_{10}	-1.6	-3.3	-0.1	-3.3	-5.6	-0.9	-2.4	-5.1	-0.9	-0.5	-3.3	2.2
$PM_{2.5}$	-2.4	-4.6	-0.8	-4.4	-7.0	-3.0	-3.0	-7.1	-1.4	-2.9	-6.5	0.6
$PM_{10-2.5}$	0.0	-2.6	3.0	-0.4	-4.2	2.3	-2.3	-4.5	0.6	0.8	-1.2	4.3
OC in PM_{10}	-0.2	-2.8	1.4	-1.0	-3.1	1.2	-0.7	-3.2	1.4	1.7	-1.3	4.0
OC in $PM_{2.5}$	-0.8	-3.7	1.4	-1.9	-3.7	0.5	-0.6	-2.8	2.1	1.5	-1.2	4.3
OC in $PM_{10-2.5}$	3.2	0.0	6.7	3.7	-1.7	7.2	-1.4	-2.5	0.1	1.2	-2.4	5.4
EC in PM_{10}	-2.8	-4.9	-0.7	-4.0	-6.0	-1.6	-5.9	-9.8	-3.3	-2.3	-9.2	0.0
EC in $PM_{2.5}$	-3.1	-5.4	-0.7	-4.6	-6.7	-3.0	-4.1	-6.7	-2.2	-2.0	-5.5	0.0
TC in PM_{10}	-1.0	-3.5	0.7	-2.0	-3.4	-0.1	-1.2	-3.6	0.9	0.9	-2.8	3.5
TC in $PM_{2.5}$	-1.4	-3.5	0.7	-2.6	-4.2	-0.9	-1.0	-3.6	1.3	0.5	-2.5	2.7
TC in $PM_{10-2.5}$	3.4	-0.3	6.7	3.1	-2.6	7.9	-1.7	-3.2	-0.7	1.1	-3.3	4.9
SO_4^{2-}	-3.0	-6.1	-0.2	-6.4	-9.0	-3.8	-4.2	-5.9	-2.9	-2.4	-5.3	0.7
SS	2.9	-1.4	7.4	1.0	-1.6	3.9	3.7	2.3	5.6	3.1	0.0	4.8
Levoglucosan[1)]	-3.3	-15.9	6.7	1.9	-6.7	5.3	-5.7	-18.1	1.4	-1.4	-12.3	7.2

Notation: Trends for levoglucosan are calculated for the period 2008–2018

.

Table S 13: Sen slope of annual mean ratios and corresponding confidence intervals for significant slopes (*p=0.05*), as well as change in annual mean presented as percentage change per year and as percentage change for the period 2001–2018 (2008–2018 for levoglucosan). Non-significant values in red.

	Slope (% yr^{-1})	CI-1	CI-2	Change 2001-2018 (%)
OC_{PM10} to PM_{10}	2.4	0.7	3.4	41
$OC_{PM2.5}$ to $PM_{2.5}$	3.2	1.7	4.4	55
$OC_{PM10-2.5}$ to $PM_{10-2.5}$	1.1	-1.3	2.5	17
EC_{PM10} to PM_{10}	-4.5	-7.1	-2.8	-77
$EC_{PM2.5}$ to $PM_{2.5}$	-3.9	-5.8	-1.9	-66
TC_{PM10} to PM_{10}	1.8	0.3	2.6	30
$TC_{PM2.5}$ to $PM_{2.5}$	2.6	1.4	3.7	44
$TC_{PM10-2.5}$ to $PM_{10-2.5}$	0.4	-1.8	1.8	7.1
SO_4^{2-} to PM_{10}	-2.1	-3.4	-0.4	-35
NO_3^- to PM_{10}	3.8	0.8	6.3	64
NH_4^+ to PM_{10}	-0.7	-3.1	2.4	-12
SS to PM_{10}	4.4	3.0	6.7	75
Levoglucosan to OC_{PM10}	-1.8	-10.6	1.8	-18
Levoglucosan to $OC_{PM2.5}$	-3.6	-9.8	1.3	-36
Levoglucosan to EC_{PM10}	2.8	-3.5	6.5	28
Levoglucosan to $EC_{PM2.5}$	2.3	-2.2	5.0	24
Levoglucosan to TC_{PM10}	-1.1	-9.0	2.7	-11
Levoglucosan to $TC_{PM2.5}$	-3.1	-8.1	2.0	-31

Notation: Trends for levoglucosan are calculated for the period 2008–2018.

Table S 14:Sen slope of seasonal mean ratios and corresponding confidence intervals for significant slopes (*p=0.05*), as well as change in annual mean presented as percentage change per year and as percentage change for the period 2001 – 2018 (2008 – 2018 for levoglucosan). Non-significant values in red.

		DJF			MAM			JJA			SON	
	Slope (% yr^{-1})	CI-1	CI-2	Slope (% yr^{-1})	CI-1	CI-2	Slope (% yr^{-1})	CI-1	CI-2	Slope (% yr^{-1})	CI-1	CI-2
OC_{PM10} to PM_{10}	1.8	-0.6	3.7	1.7	0.4	3.7	2.3	1.0	3.6	1.7	0.4	3.7
$OC_{PM2.5}$ to $PM_{2.5}$	1.8	-0.4	3.9	3.1	0.9	5.8	3.9	2.4	5.1	3.1	0.9	5.8
$OC_{PM10-2.5}$ to $PM_{10-2.5}$	2.8	-0.9	5.8	-0.3	-2.5	2.6	1.6	-1.2	3.1	-0.3	-2.5	2.6
EC_{PM10} to PM_{10}	-4.6	-7.2	-2.7	-4.7	-7.9	-2.5	-7.1	-10.7	-3.4	-4.7	-7.9	-2.5
$EC_{PM2.5}$ to $PM_{2.5}$	-3.9	-5.4	-2.5	-3.6	-5.3	-1.2	-4.3	-7.5	-1.7	-3.6	-5.3	-1.2
TC_{PM10} to PM_{10}	0.9	-1.2	3.2	1.1	-0.2	2.7	1.7	0.6	2.8	1.1	-0.2	2.7
$TC_{PM2.5}$ to $PM_{2.5}$	1.2	-0.6	3.3	-0.7	-3.6	1.6	0.7	-1.4	1.9	-0.7	-3.6	1.6
$TC_{PM10-2.5}$ to $PM_{10-2.5}$	2.2	-1.6	4.4	2.4	0.5	4.6	3.2	2.1	4.1	2.4	0.5	4.6
SO_4^{2-} to PM_{10}	-2.2	-4.0	0.1	-1.3	-3.4	-0.4	-1.3	-3.1	0.0	-1.3	-3.4	-0.4
NO_3^- to PM_{10}	7.3	3.2	11.1	1.2	-2.4	4.1	4.4	-0.4	7.1	1.2	-2.4	4.1
NH_4^+ to PM_{10}	2.6	-1.7	5.4	-1.4	-6.5	3.0	-0.6	-4.8	3.6	-1.4	-6.5	3.0
SS to PM_{10}	4.1	-0.3	7.4	4.8	1.8	7.6	6.2	4.3	8.0	4.8	1.8	7.6
Levoglucosan to OC_{PM10}	-5.9	-7.9	2.5	-4.9	-9.2	0.0	0.0	-13.6	0.0	-4.9	-9.2	0.0
Levoglucosan to $OC_{PM2.5}$	-2.7	-6.5	1.8	-4.2	-10.8	0.0	0.0	-8.7	3.7	-4.2	-10.8	0.0
Levoglucosan to EC_{PM10}	3.1	-6.9	8.6	1.1	-6.5	5.1	8.2	-2.6	13.6	1.1	-6.5	5.1
Levoglucosan to $EC_{PM2.5}$	2.5	-3.7	6.4	-0.4	-8.7	5.6	3.5	-5.1	10.7	-0.4	-8.7	5.6
Levoglucosan to TC_{PM10}	-3.5	-7.4	3.5	-5.6	-8.7	0.0	0.0	-13.6	0.0	-5.6	-8.7	0.0
Levoglucosan to $TC_{PM2.5}$	-3.2	-6.4	2.1	-2.1	-6.6	1.8	0.0	-11.9	7.4	-2.1	-6.6	1.8

Notation: Trends for levoglucosan are calculated for the period 2008–2018

Table S 15: Annual and seasonal mean mass concentrations of levoglucosan, mannosan and galactosan (2008–2018), arabitol, mannitol, trehalose, glucose, 2-methylerythritol and 2-methyltreitol (2016–2018) in PM_{10} at Birkenes. (Unit: *ng m⁻³*).

	Levo-glucosan	**Cap**	**Man-nosan**	**Cap**	**Galact-osan**	**Cap**	**Levo/ Mann**	**Cap**	**Ara-bitol**	**Cap**	**Man-nitol**	**Cap**	**2-methyl-erythritol**	**Cap**	**2-methyl-threitol**	**Cap**	**Tre-halose**	**Cap**	**Glu-cose**	**Cap**
2008	**10.90**	**90**	**2.68**	**90**	**0.91**	**90**	**4.7**	**75**												
DJF	10.24	90	2.32	90	0.69	90	4.7	69												
MAM	8.00	86	1.37	86	0.40	86	5.5	82												
JJA	13.40	86	4.48	86	2.00	90	3.4	58												
SON	11.34	97	2.63	100	0.53	97	4.5	89												
2009	**10.62**	**98**	**1.73**	**98**	**0.57**	**98**	**5.9**	**90**												
DJF	20.53	92	3.40	92	1.05	92	5.6	83												
MAM	11.84	100	1.84	100	0.69	100	6.6	100												
JJA	1.91	100	0.35	100	0.09	100	5.4	94												
SON	9.08	100	1.49	100	0.50	100	5.4	85												
2010	**17.33**	**100**	**3.89**	**100**	**1.11**	**100**	**5.2**	**85**												
DJF	43.04	100	9.39	100	2.85	100	4.9	92												
MAM	10.22	100	2.69	100	0.79	100	4.6	71												
JJA	2.96	100	1.06	100	0.11	100	5.2	84												
SON	13.71	100	2.52	100	0.73	100	5.7	92												
2011	**11.64**	100	**2.33**	**100**	**0.83**	**100**	**4.7**	**90**												
DJF	14.74	100	3.25	100	1.13	100	4,4	84												
MAM	11.79	100	2.16	100	0.94	100	5.3	92												
JJA	4.00	100	0.81	100	0.16	100	4.8	100												
SON	16.23	100	3.11	100	1.12	100	4.5	85												
2012	**10.54**	100	**2.34**	**100**	**0.73**	**100**	**4.4**	**90**												
DJF	21.75	100	4.95	100	1.43	100	4.8	100												
MAM	10.67	100	1.96	100	0.61	100	5.5	100												
JJA	1.75	100	0.65	100	0.20	100	3.2	70												
SON	8.07	100	1.82	100	0.69	100	3.8	92												
2013	**9.62**	100	**1.57**	**100**	**0.50**	**100**	**5.6**	**92**												
DJF	18.21	100	2.88	100	0.85	100	5,3	92												
MAM	10.88	100	1.81	100	0.62	100	6.7	100												
JJA	2.74	100	0.49	100	0.15	100	5.8	92												
SON	6.66	100	1.13	100	0.36	100	5.5	85												
2014	**12.78**	100	**2.99**	**100**	**0.60**	**100**	**5**	**96**												
DJF	20.14	100	4.72	100	0.92	100	4.2	92												
MAM	12.44	100	2.42	100	0.62	100	5.8	92												
JJA	3.15	100	0.56	100	0.14	100	5.8	100												
SON	16.10	100	4.47	100	0.89	100	4.1	100												
2015	**9.36**	**88**	**1.36**	**98**	**0.43**	**98**	**6.4**	**80**												
DJF	9.84	100	1.53	98	0.45	98	6.9	80												
MAM	12.31	92	1.45	92	0.63	92	6.6	61												
JJA	2.26	100	0.44	100	0.07	100	5.6	84												
SON	14.04	100	2.16	100	0.61	100	6.1	97												

	Levo-glucosan	Cap	Man-nosan	Cap	Galact-osan	Cap	Levo/Mann	Cap	Ara-bitol	Cap	Man-nitol	Cap	2-methyl-erythritol	Cap	2-methyl-threitol	Cap	Tre-halose	Cap	Glu-cose	Cap
2016	**7.52**	**97**	**1.21**	**97**	**0.30**	**94**	**5.7**	**92**	**4.78**	**99**	**3.89**	**99**	**0.38**	**99**	**0.13**	**99**	**3.17**	**99**	**5.07**	**99**
DJF	12.54	94	1.87	94	0.47	94	6.4	93	1.70	94	1.09	94	0.02	94	0.01	94	0.76	94	1.47	94
MAM	7.62	100	1.25	100	0.31	100	5.9	100	4.67	100	3.40	100	0.21	100	0.11	100	5.82	100	4.60	100
JJA	2.37	100	0.47	100	0.09	77	5.3	100	8.29	100	6.69	100	1.01	100	0.29	100	3.73	100	9.93	100
SON	7.92	92	1.30	92	0.28	100	5.5	76	4.26	100	4.17	100	0.24	100	0.09	100	2.19	100	4.04	100
2017	***8.24***	***94***	***1.35***	**95**	***0.32***	**94**	**5.6**	**92**	**5.52**	**94**	**5.70**	**94**	**0.37**	**94**	**0.10**	**94**	**3.37**	**94**	**5.17**	**94**
DJF	15.77	100	2.49	100	0.65	100	5.6	100	1.16	100	1.40	100	0.01	100	0.01	100	1.03	100	2.03	100
MAM	6.22	92	0.98	92	0.23	92	6.6	84	3.90	92	3.65	92	0.05	92	0.02	92	1.58	92	4.11	92
JJA	2.27	86	0.48	86	0.06	86	4,8	86	9.15	86	8.45	86	1.32	86	0.35	86	4.21	86	7.09	86
SON	7.84	100	1.31	100	0.29	100	5.5	100	8.18	100	9.49	100	0.17	100	0.06	100	6.61	100	7.58	100
2018	**9.77**	**100**	**1.62**	**100**	**0.39**	**100**	**6.1**	**98**	**5.76**	**100**	**5.65**	**100**	**0.45**	**98**	**0.16**	**98**	**2.83**	**100**	**4.16**	**100**
DJF	13.50	100	2.21	100	0.60	100	5.9	100	0.72	100	0.94	100	0.01	92	0.01	92	0.60	100	2.74	100
MAM	13.64	100	2.04	100	0.54	100	6.8	100	4.18	100	4.21	100	0.24	100	0.08	100	1.91	100	3.59	100
JJA	1.38	100	0.25	100	0.04	100	5.8	100	8.66	100	7.94	100	1.24	100	0.42	100	2.90	100	4.52	100
SON	10.64	100	2.01	100	0.41	100	5.5	92	9.38	100	9.47	100	0.25	100	0.12	100	5.91	100	5.79	100

Table S 16: Seasonal mean (±SD) concentrations of TC_{bb}, OC_{bb} and EC_{bb} in PM_{10} and $PM_{2.5}$ at Birkenes 2008–2018. (Unit: µg C m^{-3}).

	TC_{bb} PM_{10}	OC_{bb} PM_{10}	EC_{bb} PM_{10}	TC_{bb} $PM_{2.5}$	OC_{bb} $PM_{2.5}$	EC_{bb} $PM_{2.5}$
	TC_{bb} PM_{10}	**OC_{bb} PM_{10}**	**EC_{bb} PM_{10}**	**TC_{bb} $PM_{2.5}$**	**OC_{bb} $PM_{2.5}$**	**EC_{bb} $PM_{2.5}$**
2008	**0.160±0.042**	**0.138±0.042**	**0.021±0.005**	**0.141 ± 0.034**	**0.121 ± 0.034**	**0.020 ± 0.004**
DJF	0.150±0.039	0.130±0.039	0.020±0.004	0.133±0.032	0.114±0.032	0.019±0.004
MAM	0.117±0.031	0.102±0.030	0.016±0.003	0.104±0.025	0.089±0.025	0.015±0.003
JJA	0.196±0.05	0.170±0.051	0.026±0.006	0.174±0.042	0.149±0.042	0.025±0.006
SON	0.166±0.043	0.144±0.043	0.022±0.005	0.147±0.036	0.126±0.036	0.021±0.005
2009	**0.156±0.041**	**0.135±0.040**	**0.021±0.005**	**0.138±0.034**	**0.118±0.034**	**0.020±0.004**
DJF	0.301±0.078	0.261±0.078	0.040±0.009	0.266±0.065	0.228±0.065	0.038±0.008
MAM	0.174±0.045	0.150±0.045	0.023±0.005	0.154±0.037	0.131±0.037	0.022±0.005
JJA	0.028±0.007	0.024±0.007	0.004±0.001	0.025±0.006	0.021±0.006	0.004±0.001
SON	0.133±0.035	0.115±0.035	0.018±0.004	0.118±0.029	0.101±0.029	0.017±0.004
2010	**0.254±0.066**	**0.220±0.066**	**0.034±0.008**	**0.225±0.055**	**0.192±0.055**	**0.032±0.007**
DJF	0.631±0.164	0.547±0.164	0.084±0.019	0.558±0.136	0.478±0.136	0.080±0.018
MAM	0.150±0.039	0.130±0.039	0.020±0.004	0.132±0.032	0.113±0.032	0.019±0.004
JJA	0.043±0.011	0.038±0.011	0.006±0.001	0.038±0.009	0.033±0.009	0.006±0.001
SON	0.201±0.052	0.174±0.052	0.027±0.006	0.178±0.043	0.152±0.043	0.026±0.006
2011	**0.171±0.044**	**0.148±0.044**	**0.023±0.005**	**0.151±0.037**	**0.129±0.037**	**0.022±0.005**
DJF	0.216±0.056	0.187±0.056	0.029±0.006	0.191±0.047	0.164±0.047	0.027±0.006
MAM	0.173±0.045	0.150±0.045	0.023±0.005	0.153±0.037	0.131±0.037	0.022±0.005
JJA	0.059±0.015	0.051±0.015	0.008±0.002	0.052±0.013	0.044±0.013	0.007±0.002
SON	0.238±0.062	0.206±0.062	0.032±0.007	0.210±0.051	0.180±0.051	0.030±0.007
2012	**0.155±0.040**	**0.134±0.040**	**0.021±0.005**	**0.137±0.033**	**0.117±0.033**	**0.020±0.004**
DJF	0.319±0.083	0.276±0.083	0.043±0.009	0.282±0.069	0.241±0.069	0.040±0.009
MAM	0.156±0.041	0.136±0.041	0.021±0.005	0.138±0.034	0.118±0.034	0.020±0.004
JJA	0.026±0.007	0.022±0.007	0.003±0.001	0.023±0.006	0.019±0.006	0.003±0.001
SON	0.118±0.031	0.102±0.031	0.016±0.004	0.105±0.026	0.090±0.025	0.015±0.003
2013	**0.141±0.037**	**0.122±0.037**	**0.019±0.004**	**0.125±0.030**	**0.107±0.030**	**0.018±0.004**
DJF	0.267±0.069	0.231±0.069	0.036±0.008	0.236±0.058	0.202±0.058	0.034±0.008
MAM	0.159±0.041	0.138±0.041	0.021±0.005	0.141±0.034	0.121±0.034	0.020±0.004
JJA	0.040±0.010	0.035±0.010	0.005±0.001	0.035±0.009	0.030±0.009	0.005±0.001
SON	0.098±0.025	0.085±0.025	0.013±0.003	0.086±0.021	0.074±0.021	0.012±0.003
2014	**0.187±0.049**	**0.162±0.049**	**0.025±0.006**	**0.166±0.040**	**0.142±0.040**	**0.024±0.005**
DJF	0.295±0.077	0.256±0.077	0.040±0.009	0.261±0.064	0.224±0.064	0.037±0.008
MAM	0.182±0.047	0.158±0.047	0.024±0.005	0.161±0.039	0.138±0.039	0.023±0.005
JJA	0.046±0.012	0.040±0.012	0.006±0.001	0.041±0.010	0.035±0.010	0.006±0.001
SON	0.236±0.061	0.204±0.061	0.032±0.007	0.209±0.051	0.179±0.051	0.030±0.007
2015	**0.137±0.036**	**0.119±0.036**	**0.018±0.004**	**0.121±0.030**	**0.104±0.030**	**0.017±0.004**
DJF	0.144±0.038	0.125±0.038	0.019±0.004	0.128±0.031	0.109±0.031	0.018±0.004
MAM	0.180±0.047	0.156±0.047	0.024±0.005	0.160±0.039	0.137±0.039	0.023±0.005
JJA	0.033±0.009	0.029±0.009	0.004±0.001	0.029±0.007	0.025±0.007	0.004±0.001
SON	0.206±0.054	0.178±0.054	0.028±0.006	0.182±0.044	0.156±0.044	0.026±0.006
2016	**0.110±0.029**	**0.096±0.029**	**0.015±0.003**	**0.098±0.024**	**0.084±0.024**	**0.014±0.003**
DJF	0.184±0.048	0.159±0.048	0.025±0.005	0.162±0.040	0.139±0.040	0.023±0.005
MAM	0.112±0.029	0.097±0.029	0.015±0.003	0.099±0.024	0.085±0.024	0.014±0.003

	TC_{bb} PM_{10}	**OC_{bb} PM_{10}**	**EC_{bb} PM_{10}**	**TC_{bb} $PM_{2.5}$**	**OC_{bb} $PM_{2.5}$**	**EC_{bb} $PM_{2.5}$**
JJA	0.035±0.009	0.030±0.009	0.005±0.001	0.031±0.007	0.026±0.007	0.004±0.001
SON	0.116±0.030	0.101±0.030	0.016±0.003	0.103±0.025	0.088±0.025	0.015±0.003
2017	**0.121±0.031**	**0.105±0.031**	**0.016±0.004**	**0.107±0.026**	**0.092±0.026**	**0.015±0.003**
DJF	0.231±0.060	0.200±0.060	0.031±0.007	0.204±0.050	0.175±0.050	0.029±0.007
MAM	0.091±0.024	0.079±0.024	0.012±0.003	0.081±0.020	0.069±0.020	0.012±0.003
JJA	0.033±0.009	0.029±0.009	0.004±0.001	0.029±0.007	0.025±0.007	0.004±0.001
SON	0.115±0.030	0.100±0.030	0.015±0.003	0.102±0.025	0.087±0.025	0.015±0.003
2018	**0.143±0.037**	**0.124±0.037**	**0.019±0.004**	**0.127±0.031**	**0.108±0.031**	**0.018±0.004**
DJF	0.198±0.052	0.171±0.051	0.026±0.006	0.175±0.043	0.150±0.043	0.025±0.006
MAM	0.200±0.052	0.173±0.052	0.027±0.006	0.177±0.043	0.151±0.043	0.025±0.006
JJA	0.020±0.005	0.018±0.005	0.003±0.001	0.018±0.004	0.015±0.004	0.003±0.001

Table S 17: Equations showing the relationship between EC, OC and TC for ambient $PM_{2.5}$ aerosol filter samples collected at Birkenes in 2014, obtained by temperature calibrated Quartz and EUSAAR-2 temperature programs.

EC	$EC_{EUSAAR\text{-}2,\ TOT} = EC_{QUARTZ,\ TOT} \times 1.6118$	$R^2 = 0.876$	n = 50	Eq. S 16
OC	$OC_{EUSAAR\text{-}2,\ TOT} = OC_{QUARTZ,\ TOT} \times 0.8687$	$R^2 = 0.977$	n = 50	Eq. S 17
TC	$TC_{EUSAAR\text{-}2,\ TOT} = TC_{QUARTZ,\ TOT} \times 0.9151$	$R^2 = 0.976$	n = 50	Eq. S 18